Mater. Res. Soc. Symp. Proc. Vol. 1415 © 2012 Materials Research Society
DOI: 10.1557/opl.2012.72

Ti-TiO_x-Pt Metal-Oxide-Metal Diodes Fabricated via a Simple Oxidation Technique

Linzi E. Dodd[1], Andrew J. Gallant[1], David Wood[1]
[1]School of Engineering and Computing Sciences, Durham University
Science Laboratories, South Road, Durham, DH1 3LE, United Kingdom

ABSTRACT

This work presents the successful production, via a simple oxidation process, of Ti-TiO_x-Pt Metal-Oxide-Metal diodes with excellent electrical asymmetry. TEM analysis has been used to verify the oxide thickness. A thicker layer produces better diodes, although they are of a less uniform nature. The conduction mechanism in these diodes is still under investigation.

INTRODUCTION

Energy recovery systems have attracted much interest in recent years [1-3]. A significant amount of energy is wasted in the form of heat, leading to research dedicated specifically to energy recovery from this source. In electromagnetic terms, heat is infrared radiation, and its energy content will follow Planck's Law of spectral distribution. The wavelength of maximum emission intensity λ_{max} within this distribution can be calculated using Wien's Law (Eqn. 1):

$$\lambda_{max} T = 2.897 \times 10^{-3} \text{ m.K} \quad (1)$$

An application example is for heat energy recovery from automotive exhaust pipes. Typical internal combustion engines are only 25-30% efficient. Around 40% of the waste is lost as heat in exhaust gases, with 10-20% of this being radiated through the exhaust pipe surface [4]. For an automobile at a cruising speed, this means a typical value in the range of 10-30 kW is lost through exhaust pipe radiation – we have confirmed these calculations with thermal camera analysis.

As a result of increasing pressure on automobile manufacturers to make their products more efficient, a significant amount of research is being undertaken into energy recovery systems. An antenna array, with rectifying diodes, could provide a cost effective, scaleable, high efficiency solution to the issue of energy recovery. In the temperature range of 500-1000 K, Eqn. 1 gives a wavelength of ~3-6 μm, or in frequency terms ~50-100 THz. This is extremely challenging for the rectifying capability of any diode technology. Metal-Oxide-Metal (MOM) structures, with electron tunneling as the transport mechanism, [5-6], are the most promising type of diode to use in this application. The diode itself consists of two dissimilar metals, separated by a uniform native oxide layer, which is sufficiently thin to allow electron tunneling to occur, i.e. is <5 nm thick. A functional diode is best achieved by using one metal which will oxidize readily and another which is inert. The asymmetry of the diode can be increased by maximizing the work function difference between these metals, and here we have chosen titanium and platinum to give a difference of 1.4 eV.

EXPERIMENTAL DETAILS

Fabrication

The fabrication process is shown in Fig. 1. N-type <100> silicon of 10-30 Ωcm resistivity was chosen as the substrate material (2" diameter wafers) and was oxidized to provide an

insulating 1000 Å film. A bi-layer lift-off process, using PMGI SF9 and Microposit SPR-350 photoresists, an EVG 620 mask aligner and MF-319 developer, was then used to produce a base layer pattern on the wafer, on top of which 25 nm of titanium and 100 nm of gold were deposited in the same e-beam evaporation process (Fig. 1a, with the silicon substrate not shown for overall clarity). The photoresist was removed using 1165 stripper.

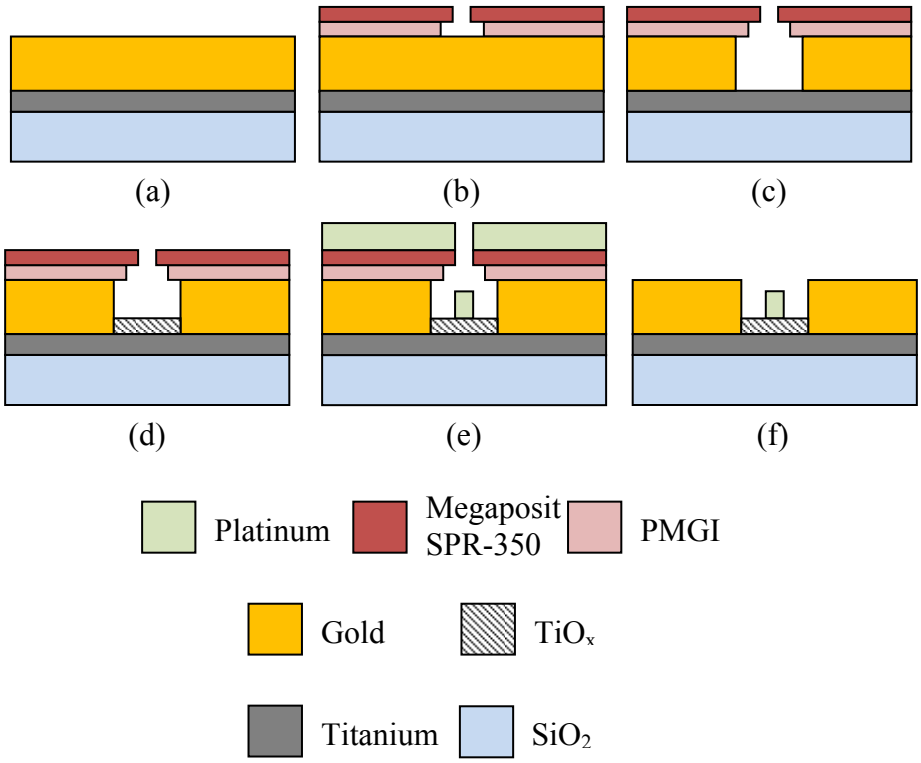

Figure 1 – Fabrication process of MOM diode.

The lift-off process was repeated, as in (b), and then an etchant (4:1:8 KI:I_2:H_2O) was used to remove the uncovered gold and to undercut the photoresist, leaving a small region of titanium exposed (c). The samples were then placed in an ultrasonic bath in water for 10 seconds to help remove any remaining gold etch solution. The exposed titanium was oxidized using the techniques described below and then immediately placed in the e-beam evaporator. 30 nm of platinum was then evaporated, resulting in a small Ti/TiOx/Pt region being produced (e). Finally, the photoresist was removed as above, which also removed unwanted platinum, completing the diode fabrication process (f).

Oxidation Techniques

Various oxidation techniques have been used to produce a sufficiently thin oxide, ranging from exposure to ambient environment, to the controlled etching and regrowth of an oxide via reactive ion etching (RIE). However, for this set of diodes, oxidation occurred via exposure to a moist elevated temperature environment for varying lengths of time. The resulting oxides and their rectification characteristics are discussed below.

RESULTS AND DISCUSSION

FIB Analysis of Diode

Once produced, the diodes were tested for their electrical performance. Specimens of each diode were then further processed using a FIB and subsequent TEM analysis. Figure 2 shows a FIB image of one of the diode cross-sections, where the horizontal line is titanium/gold, and the vertical line is platinum, with the central crossover denoting the diode itself. Currently, we have made diodes with dimensions down to 10 x 10 μm, but future work will extend this to sub-200 nm dimensions.

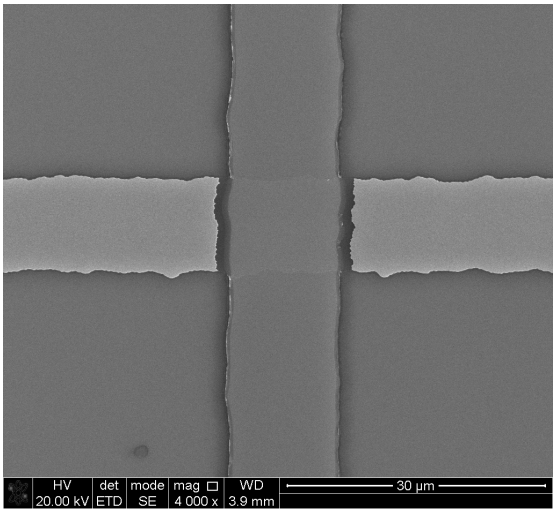

Figure 2 – FIB image of diode cross-section.

Diode Operation

Details of the test and analysis procedure have been published previously [7]. A typical I-V plot is shown in Figure 3, where the asymmetric diode characteristics can be seen clearly. The often quoted figure of merit for these devices, curvature coefficient (CC), is plotted against voltage in Figure 4. As is often the case, the highest value of curvature is away from the ideal value of zero bias. Nevertheless, the typical values of CC obtained from these $Ti/TiO_x/Pt$ diodes (5.5 V^{-1} at zero bias) are very competitive when compared with results published from other metallization systems [8].

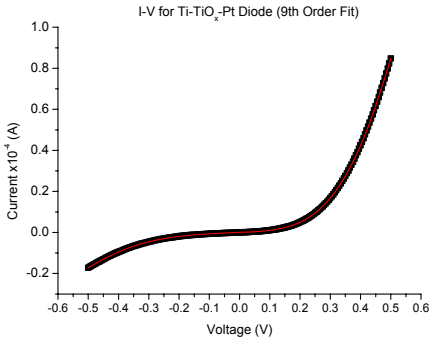

Figure 3 – I-V curve for a typical diode.

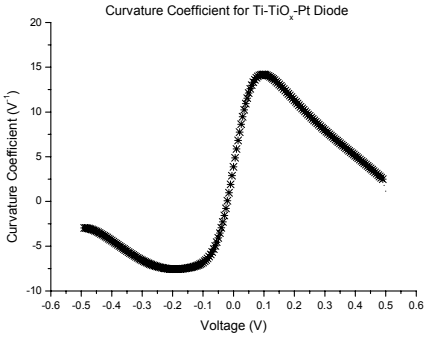

Figure 4 – CC vs. voltage for a typical diode.

TEM Analysis

TEM analysis of sample diodes was used to determine the nature of the native titanium oxide grown via wet furnace oxidation. Figure 5 shows a dark field image of two diode cross-sections, where both the collimated structure of the titanium metal, and the titanium oxide above it, can be seen clearly. The 2 hour oxide is on average 6 nm thick, whereas a 4 hour oxide is thicker at 7.6 nm on average.

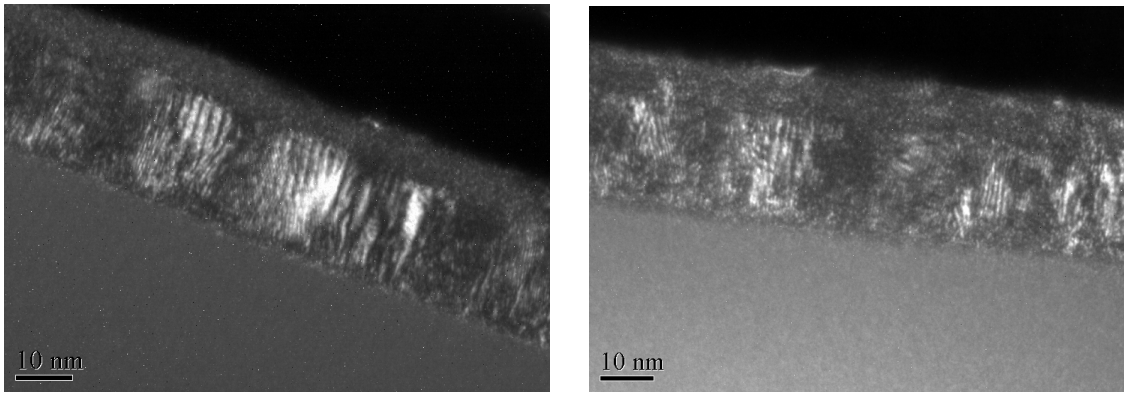

Figure 5 - Dark field TEM image of (bottom to top) SiO_2, Ti, TiO_x, and Pt (appears black here) (2 hour oxide on left, 4 hour oxide on right).

Figure 6 shows two high resolution images of the titanium layers and their native oxides. Again the collimated structure of the titanium can be seen, in contrast to the native oxide. The variations in oxide thickness can also be seen, particularly in the 4 hour oxide layer, which may help explain our observations of variable electrical performance of subsequent diodes. In contrast, the thinner oxide layer produces more uniform electrical results.

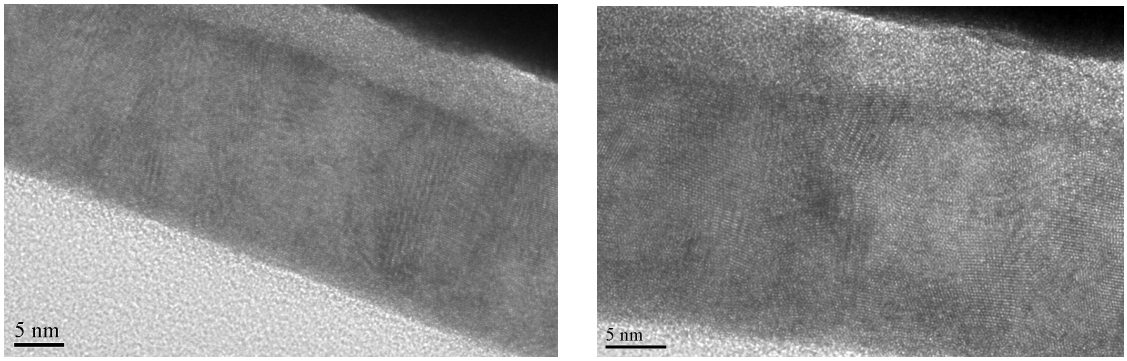

Figure 6 - HREM image of the titanium and titanium oxide layers of a MOM diode (2 hour oxide on left, 4 hour oxide on right).

RBS Analysis

RBS analysis has been undertaken on a range of samples with different oxidation regimes. As measured immediately after deposition, results suggest a 2-3 nm thick oxide grows immediately on a titanium layer. From there, the results are more ambiguous: despite trying a range of oxide preparation times, we were unable to detect any conclusive increase in the oxide

thickness. These results are at odds with the electrical results, and typical TEM images, which are influenced by oxide preparation time. We attribute the RBS results to our working at the limits of the sensitivity of the equipment. We are currently investigating other surface analysis techniques, including TOF-SIMS (Time of Flight Secondary Ion Mass Spectrometry), to elucidate both the thickness and the stoichiometry of the oxide under different preparation conditions.

The Effects of Oxide Thickness on Diode Performance

Diodes which have been produced with a 4 hour oxidation process have much higher curvature coefficients and larger resistances than the 2 hour oxidation diodes, but their values are less uniform. Figure 7 shows a comparison between the peak curvature coefficient of the 2 hour diodes and the zero bias curvature coefficient of the 4 hour diodes. As plotted by wafer position, the 4 hour diodes are much more useful at zero bias, whereas the thinner oxides appear to require biasing in order to show rectification qualities. These results are perhaps at first surprising, given the slight difference in oxide thickness between the two oxidation regimes, but they are consistent. The more uniform electrical results for a thinner oxide could be a result of a more uniform oxide, but we are at present unable to confirm this. The yield is also lower for these devices, which may simply be due to the increased difficulty in distinguishing operational diodes. Given the values of the measured oxide thickness, it is clear that the transport mechanism is more involved than first thought: an oxide thickness <5 nm is considered to be the limit for tunneling MOM diodes. Work is ongoing to find a compromise which provides an oxide that is of the required thickness and uniformity, which allows favorable curvature values in the diodes, and also which enables us to determine the current carrying mechanism(s).

	10	10	12	12	14	14	16	16	
	8	9	8	9	8	9	8	9	
10	0.4	0.2	0.2	0.2	0.5	0.2	0.3	0.2	10
10	0.5	0.7	0.2	-	-	-	-	-	10
10	0.2	0.4	0.2	-	0.4	-	0.3	0.6	10
10	0.3	0.3	-	0.3	0.7	-	0.4	0.5	10
10	0.4	0.6	-	-	0.6	-	0.4	-	10
10	0.6	0.6	0.3	0.2	0.2	-	-	0.1	10
10	0.6	-	-	0.4	0.2	0.6	0.3	0.6	10
10	0.2	0.4	0.2	-	0.3	0.2	0.9	0.6	10
	1	16	1	16	1	16	1	16	
	10	10	12	12	14	14	16	16	

	10	10	12	12	14	14	16	16	
	8	9	8	9	8	9	8	9	
10	-	3.6	3.1	2.3	3.3	3.5	3.1	4.0	10
10	1.5	2.6	2.0	2.4	3.9	5.8	2.5	1.8	10
10	1.9	3.4	2.2	1.8	3.4	3.7	4.3	0.5	10
10	3.7	3.2	3.8	5.0	5.0	3.5	-	1.1	10
10	2.3	3.3	4.2	4.4	3.7	2.7	4.3	6.8	10
10	5.4	0.3	3.3	3.3	3.5	2.6	2.0	1.7	10
10	3.0	3.1	3.0	3.4	3.7	1.5	3.2	2.4	10
10	0.8	1.7	3.9	3.8	3.2	3.9	1.2	1.7	10
	1	16	1	16	1	16	1	16	
	10	10	12	12	14	14	16	16	

Figure 7 – Peak curvature of a 2 hour oxide diode (left), and zero bias curvature of 4 hour oxide (right).

CONCLUSIONS

MOM diodes have been produced, with different electrical properties based on the duration of their oxidation. The thickest oxide is in the region of 7.6 nm thick by TEM, which produced high performance diodes. A slightly thinner oxide gave lower values of both curvature coefficient and resistance. Based on the uniformity of these values, it was believed that the thinner oxide is more uniform. We are still investigating why these diodes show such good

characteristics, as it is commonly thought that for electron tunneling to occur the oxide needs to be much thinner. A clearer understanding of the variations in uniformity and stoichiometry (leading to alternative and/or parallel conduction mechanisms) will be needed to elucidate an explanation.

ACKNOWLEDGMENTS

The authors wish to thank Dr Mark Rosamond and Mr Leon Bowen for their assistance preparing samples using the FIB, Dr Budhika Mendis for the TEM images and finally Dr Richard Thompson for the RBS analysis.

REFERENCES

1. J. A. Bean, A. Weeks and G. D. Boreman, "Performance optimization of antenna-coupled Al/AlOx/Pt tunnel diode infrared detectors", *IEEE J. Quantum Electron.* **47**, 126-135, (2011)
2. M. Dagenais, K. Choi, F. Yesilkoy, A. N. Chryssis and M. C. Peckerar, "Solar spectrum rectification using nano-antennas and tunneling diodes", Optoelectronic Integrated Circuits, San Francisco, USA, January 27-28, 2010*, Proc. SPIE* **7605**, 76050E, (2010)
3. J. Alda, J. M. Rico-García, J. M. López-Alonso and G. Boreman, "Optical antennas for nano-photonic applications", *Nanotechnology*, **16**, S230-S234, (2005)
4. F. Stabler, "Automotive thermoelectric generators: design & manufacturing", *Proc. MRS Spring Meeting, San Francisco, USA*, April 13-17, 2009, Symposium N: Materials and Devices for Thermal-to-Electric Energy Conversion
5. K. M. Evenson, D. A. Jennings and F. R. Peterson, "Tunable far-infrared spectroscopy", *Appl. Phys. Lett.*, **44**, 576-578, (1984)
6. S. P. Kwok, G. I. Haddad and G. Lobov, "Metal-Oxide-Metal (M-O-M) Detector", *J Appl. Phys.*, **42**, 554-563, (1971)
7. L. E. Dodd, D. Wood and A. J. Gallant, "Optimizing MOM Diode Performance via the Oxidation Technique", *Proc. IEEE Sensors 2011*, Limerick, Ireland, 28-31 October, 2011, 176-179
8. B. Tiwari, J. A. Bean, G. Szakmany, G. H. Bernstein, P. Fay and W. Porod, "Controlled etching and regrowth of tunnel oxide for antenna-coupled metal-oxide-metal diodes", *J Vac. Sci. Technol.*, **27**, 2153-2160, (2009)